HHS Public Access

Author manuscript

Dev Biol. Author manuscript; available in PMC 2023 May 25.

Published in final edited form as:

Dev Biol. 2022 November ; 491: 113–125. doi:10.1016/j.ydbio.2022.09.001.

Developmental regulation of epithelial cell cuboidal-to-squamous transition in *Drosophila* follicle cells

Dongyu Jia[1,2,*,#], **Allison Jevitt**[2,3,#], **Yi-Chun Huang**[4], **Belen Ramos**[1], **Wu-Min Deng**[2,4,*]

[1]Department of Biology, Georgia Southern University, Statesboro, GA, 30460, USA

[2]Department of Biological Science, Florida State University, Tallahassee, FL 32306-4370, USA

[3]Cell Cycle and Cancer Biology Program, Oklahoma Medical Research Foundation, Oklahoma City, OK 73104, USA

[4]Department of Biochemistry and Molecular Biology, Tulane Cancer Center, Tulane University School of Medicine, New Orleans, LA, USA

Abstract

Epithelial cells form continuous membranous structures for organ formation, and these cells are classified into three major morphological categories: cuboidal, columnar, and squamous. It is crucial that cells transition between these shapes during the morphogenetic events of organogenesis, yet this process remains poorly understood. All three epithelial cell shapes can be found in the follicular epithelium of *Drosophila* egg chamber during oogenesis. Squamous cells (SCs), are initially restricted to the anterior terminus in cuboidal shape. They then rapidly become flattened to assume squamous shape by stretching and expansion in twelve hours during midoogenesis. Previously, we reported that Notch signaling activated a zinc-finger transcription factor Broad (Br) at the end of early oogenesis. Here we report that ecdysone and JAK/STAT pathways subsequently converge on Br to serve as an important spatiotemporal regulator of this dramatic morphological change of SCs. The early uniform pattern of Br in the follicular epithelium is directly established by Notch signaling at stage 5 of oogenesis. Later, ecdysone and JAK/STAT signaling activities synergize to suppress Br in SCs from stage 8 to 10a, contributing to proper SC squamous shape. During this process, ecdysone signaling is essential for the SC stretching, while JAK/STAT regulates SC clustering and cell fate determination. This study reveals an inhibitory role of ecdysone signaling in suppressing Br in epithelial cell remodeling. In this study we also used single-cell RNA sequencing data to highlight the shift in gene expression which occurs as Br is suppressed and cells become flattened.

[*]Correspondence: Wu-Min Deng (Tel: 504-988-5289; wdeng7@tulane.edu) Dongyu Jia (Tel: 912-478-5664; Fax: 912-478-0845; djia@georgiasouthern.edu).

[#]Equal contribution

Author Contributions

D.J. designed the project, performed the experiments, analyzed the data, made the figures, drafted and revised the paper; A.J. created the diagrams, co-drafted the paper and revised the paper; A.J. and Y.C.H. contributed to data collection and analysis; B.R. contributed to the data collection for the manuscript revision; W.M.D. revised the paper and supervised the project. All authors approved the manuscript for submission.

Competing Interests

The authors have declared that no competing interests exist.

Keywords

Ecdysone; JAK/STAT; Notch; broad; follicle cells; egg chamber; stretched cells; squamous cells

Introduction

Morphogenesis of developing organisms occurs through the coordination of shape changes in all tissues. One tissue type, the epithelium, is especially important in separating body cavities, lining the blood vessels, and mediating the secretion and absorption of chemicals, all while providing a protective physical barrier for vital organs (Mateo et al., 2015). The specialized function of these epithelial tissues depends on their characteristic structure. Complex tissue shape changes like invagination, convergence, extension, and flattening, contribute to epithelial tissue morphogenesis and are driven by the additive shape changes of individual adherent epithelial cells (Keller et al., 2003). There are three basic shapes which an epithelial cell can assume: cuboidal, columnar, and squamous. These categories are based on the proportions of the cell, wherein cuboidal cells have equal height and width, columnar cells have a greater height than width, and squamous cells have a greater width than height (Schock and Perrimon, 2002).

Epithelial cell shape changes are highly organized in development. Its regulation of morphogenesis is mainly through two mechanisms, one is pulsatile and transient flow, and another is mechanically-linking cells via supracellular cables (Miao and Blankenship, 2020). The former is always associated with actomyosin networks, a transient imbalance of which can lead to a dynamic morphological change. From transient activation to lasting changes, highly orchestrated cell signaling pathways play important roles in regulating the unidirectional changes. This has recently been an area of intense focus and as a result many involved signaling pathways have been reported. For example, G protein-coupled receptors (GPCRs)-based signaling can activate Myosin II and Rho Kinase at the apical side to initiate pulsative actomyosin flows, which results in cell shape changes (Kerridge et al., 2016). In insects, the steroid hormone ecdysone is well-known for its role in triggering the larval-to-adult metamorphosis, which involves dramatic morphological changes (Thummel, 1996). Broad is a major early ecdysone-inducible gene to further induce secondary-response genes to regulate the metamorphosis (Karim et al., 1993).

The *Drosophila* egg chamber is an excellent model for studying not only signaling pathways in development (Assa-Kunik et al., 2007; Boyle and Berg, 2009; Buszczak et al., 1999; Deng et al., 2001; Ghiglione et al., 2008; Klusza and Deng, 2011; Nilson and Schupbach, 1999; Roth and Lynch, 2009; Tian et al., 2013), but also morphogenetic movements including cell migration, tissue elongation, and epithelial rotation (Grammont, 2007; Montell et al., 2012; Osterfield et al., 2015; Peters and Berg, 2016; (Cetera et al., 2014; Haigo and Bilder, 2011). Each egg chamber consists of sixteen germline cells (fifteen nurse cells and one oocyte) enveloped by a monolayered epithelium made up of somatic follicle cells. Fully formed egg chambers pinch off from the germarium and move posteriorly in a queue. This development is subdivided into 14 stages based on morphological characteristics (Jia et al., 2016; Spradling, 1993). Early-stage egg chambers contain only two types of

follicle cells: the polar cells at the anterior and posterior termini of the egg chamber (Besse and Pret, 2003; Shyu et al., 2009) and the cuboidal-shaped main-body follicle cells (MbFCs), which maintain an immature cell fate and undergo mitotic cycles until stage 5. Notch signaling activation triggers the differentiation and the mitotic to endocycle switch of these MbFCs (Klusza and Deng, 2011). Afterward, the majority of the MbFCs transition from cuboidal to columnar shape, whereas around sixty follicle cells at the anterior are further differentiated into the border cells (BCs) and the squamous cells (SCs, also known as stretched cells), upon receiving the polar cell-secreted Upd signaling. Concomitantly with the cell fate change, newly differentiated SCs transition from cuboidal to squamous shape to accommodate the growing nurse cells (Kolahi et al., 2009). During the process, the anterior SCs stretch towards the posterior and expand to cover the enlarged anterior volume of egg chamber, meanwhile the adjacent MbFCs also migrate to the posterior to cede more covering surface area to SCs (Figure 1). Finishing the cuboidal-to-squamous transition at stage 10a, approximately fifty SCs spread over the nurse cells, fully covering the anterior half of the egg chamber, meanwhile MbFCs cover the other half volume at the posterior (Figure 1). In addition, follicle cells undergo collective movement from stage 5 to stage 9 to rotate the egg chamber within its surrounding basement membrane, and this process is important for the egg chamber elongation (Cetera et al., 2014; Haigo and Bilder, 2011).

From stage 8 to stage 10, the cuboidal-to-squamous cell transition (referred to here as cell flattening) results in an anterior epithelial layer in which the cells are remodeled to be highly flattened and spread out. It has been reported that the gene *Tao* controls SC flattening by promoting Fasciclin 2 endocytosis (Gomez et al., 2012). Two signaling pathways, Notch and Transforming Growth Factor β, remodel adherens junctions to induce SC flattening during *Drosophila* oogenesis (Brigaud et al., 2015; Grammont, 2007). While studies have revealed some important molecules that can modify cell shape and those which are especially crucial in flattening, the genetic control of this dynamic and complicated SC shape change remains less known.

In this report, we utilized *Drosophila* egg chamber SCs as the model system to study the mechanisms underlying SC flattening. Previously, we demonstrated that the early uniform pattern of Broad (Br), a small group of zinc-finger transcription factors resulting from alternative splicing, is established in the follicular epithelium by Notch signaling at stage 5 during *Drosophila* oogenesis (Jia et al., 2014). Here, we report that downregulation of Br in SCs from stage 9 to 10a is critical for proper SC flattening. Both ecdysone and JAK/STAT signaling mediate the downregulation of Br. Therefore, Br acts downstream of the Notch, ecdysone, and JAK/STAT pathways, thus serving as an important spatiotemporal cue for proper cell flattening. In addition, we confirmed the upregulation of other ecdysone and JAK/STAT signaling components during the transition from MbFCs to SCs, especially those mutually exclusive to Br.

Results

The expression of Br gradually disappears in SCs and BCs from stage 9.

Previously, using a Br-core antibody (Emery et al., 1994) we found that Br expression was activated by Notch signaling at stage 5 during oogenesis, and was present in all follicle

cells until stage 8 with the exception of the polar cells (Jia et al., 2014; Rowe et al., 2020). To identify the Br expression pattern during SC flattening, we stained Br in flies carrying A90-Gal4, which is expressed specifically in anterior follicle cells, including SCs and BCs, from stages 6/7 (Tran and Berg, 2003). Using A90-Gal4 driven mRFP as an indicator, we found that SCs initiate flattening at early stage 9, and become entirely flattened by stage 10a to cover the increased germline surface area (Figure 1A–D). In early stage 9, Br expression is reduced in the BCs, and SCs as they begin to undergo the cuboidal-to-squamous cell transition. By stage 10a, fully flattened SCs have lost Br completely. During this gradual decrease of Br from stage 9–10, the MbFCs maintain high Br expression, comparable to their levels during stage 8 (Figure 1). The disappearance of Br expression in the SCs raises some interesting questions, including the significance and the genetic regulations of Br downregulation, and the relevance of Br disappearance concurrent with the flattening of SCs.

Misexpression of Br causes SC stretching defects.

The nuclei of SCs are spaced out over the anteriorly-located nurse cells, occupying half the volume of the egg chamber at stage 10. Most SC nuclei are located in the hexagonal-shaped interstitial gaps between nurse cells (Figure 2A). To understand the relationship between Br downregulation and SC flattening, we first used the flip-out Gal4/UAS technique (Pignoni and Zipursky, 1997) to misexpress Br-Z1, the most abundant Br isoform during oogenesis (Tzolovsky et al., 1999). In the anterior end of the egg chamber, Br misexpression resulted in stretching defects in which SCs accumulated instead of proper flattening and stretching apart (Figure 2B). However, the flip-out clones were generated mainly during the mitotic stages of oogenesis (stages 1–5), during which time the misexpression of Br could potentially have interfered with the differentiation of the SCs. If this were true, the stretching defects would have resulted from the cells maintaining an immature follicle cell fate rather than from disturbance of the mechanism of flattening in fully-fated SCs. To circumvent the potential early effect, we applied the SC-driver, A90-Gal4, which is specifically expressed in SCs during mid-oogenesis, following the adoption of SC fate (Tran and Berg, 2003). Consistent with the above-mentioned flip-out results (Figure 2B), A90-driven Br-misexpressing SCs also failed to stretch and disperse (Figure 2C). The SC flattening defects were alleviated by introducing *br* RNAi into the Br-misexpressing SCs (Figure 2E), further suggesting that Br downregulation is important for proper SC stretching and dispersion. Interestingly, we also found the MbFCs migrated slower than usual, failing to reach the posterior half of the A90-Gal4/UAS-Br-Z1 egg chambers at stage 10a (Figure 2C”), indicating communication may be required between SCs and MbFCs to coordinate morphogenetic movement. In contrast, when ptc-Gal4, which is expressed specifically in MbFCs after stage 8 (Tamori and Deng, 2013), was used to overexpress Br-Z1 in MbFCs, neither SC stretching nor MbFC migration was affected (Figure 2D). Together, these results suggest downregulation of Br is specifically required in SCs for proper SC flattening.

Ecdysone signaling downregulates Br in SCs.

Br is well known as a key downstream target of ecdysone to regulate metamorphosis in *Drosophila* (Mugat et al., 2000). The timing of another morphogenetic movement, BC migration, is controlled by ecdysone signaling during stage 9. The ecdysone receptor

isoform, which is required for BC migration (EcR-B1), is also present in the SCs from stage 8 (Jang et al., 2009). This suggests that ecdysone signaling might be involved in regulating SC morphogenesis as well. We examined the expression pattern of the ecdysone signaling reporter, *EcRE-lacZ* (Koelle et al., 1991; Kozlova and Thummel, 2003), and found ecdysone activity initiates from the anterior-most SCs at stage 8, then extends progressively towards posteriorly-located SCs, complementary to the expression pattern of Br (Figure 3A). At stage 10a, high levels of ecdysone activity were observed in SCs, while no Br was detected (Figure 3B). This observation is highly interesting because Br has been reported as a positively regulated target of ecdysone in all previous publications. Our findings suggest that ecdysone downregulates Br during SC flattening.

To investigate whether ecdysone activity is required for proper SC flattening and Br downregulation, we blocked EcR-B1 activity using the flip-out Gal4 to express a dominant negative construct *UAS-EcR-B1 W650A* (abbreviated *UAS-EcR-B1* ^{DN}) (Brown et al., 2006; Cherbas et al., 2003; Hu et al., 2003; Schubiger et al., 2005). The dominant negative (DN) form of EcR-B1 loses the ability to bind ligand properly; thus, its overexpression acts as a competitive inhibitor of wild-type EcR-B1 and represses ecdysone function. SCs with misexpression of EcR-B1^{DN} failed to stretch and disperse properly (Figure 3C). Meanwhile, upregulated Br expression was observed in these defective SCs (Figure 3C), suggesting ecdysone signaling is important for SC flattening and downregulation of Br. Repression of EcR-B1 function driven by A90-Gal4 in SCs caused cells to accumulate at the anterior (Figure 3D), indicating ecdysone signaling is essential for SC stretching and dispersion. In contrast, repressing EcR-B1 function in MbFC using ptc-Gal4 did not affect SC flattening, and MbFC migration (Figure 3E), confirming ecdysone signaling specifically suppresses Br in SCs for proper cuboidal-to-squamous transition. Introduction of *br* RNAi into the EcR-B1-suppressed SCs alleviated cell accumulation defects (Figure 3F), indicating ecdysone signaling regulates proper SC flattening via downregulation of Br. Statistical quantification and analysis through measuring the Accumulation Percentage (see Methods) further supported our claim that impaired ecdysone signaling results in SCs accumulating at the anterior, and downregulation of Br in these ecdysone-suppressed cells reduces the accumulation of SCs (Figure 3G, 3H).

The stretching defects observed in the EcR-B1^{DN} SCs differed from that of the Br-Z1 SCs in that the EcR-B1^{DN} SC layer appeared to be no longer contiguous. To investigate this further, we stained for the cell adhesion molecule Armadillo (Arm) to test if the loss of stretching due to EcR-B1^{DN} may also increase cell adhesion (Figure 4). When comparing Arm staining between Br-Z1 and EcR-B1^{DN} SC defects, we found low levels of Arm in the Br-Z1-misexpressing SCs, despite their lack of stretching (Figure 4C, 4D). Conversely, EcR-B1^{DN} SCs had accumulated Arm (Figure 4E, 4F). This may explain the large holes in the SC layer (Figure 4E', 4F') which could result from tighter cell-cell contact and a stiffer, less compliant epithelium which tears as the germline beneath it grows. Despite this difference in adhesion levels between Br-Z1 and EcR-B1^{DN} conditions, in both cases, SCs did not attain squamous cell shape as demonstrated by images of the midsagittal plane. Cells appeared more cuboidal with less space between nuclei and a greater cell height than control SCs (Figure 4A"-4F").

At stage 10a, Br is not detected in fully stretched SCs, while highly expressed in MbFCs (Figure 1D). We found the expression of ecdysone activity reporter *EcRE* was highly upregulated in *br* mutant MbFCs, while it was undetectable in neighboring wild-type cells (Figure 5A), indicating Br possesses the ability to suppress ecdysone signaling. Similarly, knockdown of *br* in the SCs increased *EcRE* expression levels (Figure 5B), confirming Br feeds back to suppress ecdysone activity in SCs as well. Basically, Br and ecdysone mutually suppress each other's expression. While strong ecdysone signaling suppresses Br in SCs, strong Br dominates in the MbFCs.

JAK/STAT signaling downregulates Br in SCs.

Gradient JAK/STAT signaling has been implicated in the anterior cell fate determination and morphological changes. Similar to ecdysone, JAK/STAT signaling has been known to mobilize BCs during BC migration (Montell et al., 2012). We hypothesized that JAK/STAT may also aid SCs in their shape transition from cuboidal to squamous. We found that JAK/STAT signaling reporter 10XSTAT92E-GFP (abbreviated 10XSTAT-GFP) (Bach et al., 2007) was highly expressed at the anterior-most SCs at stage 9, in contrast to the decreased expression pattern of Br (Figure 6A). In addition, during stage 10a, moderate levels of JAK/STAT activity were still observed in fully flattened SCs lacking Br (Figure 6B). The expression pattern of JAK/STAT activity indicates that JAK/STAT signaling might also play a similar regulatory role to the EcR pathway in regulating SC flattening through the repression of Br.

We then used the flip-out Gal4/UAS technique to knock down JAK/STAT signaling in order to investigate the role of JAK/STAT activity for proper SC flattening through the downregulation of Br. Similar to the Br-Z1 misexpression phenotype, SCs with JAK/STAT knockdown failed to stretch and disperse properly and showed upregulated levels of Br (Figure 6 C), suggesting that JAK/STAT signaling participates in the downregulation of Br and is important for SC flattening. Downregulation of JAK/STAT driven by A90-Gal4 in SCs caused cells to form clusters, and weakly elevated Br expression (Figure 6D), while downregulation of JAK/STAT in MbFCs did not affect SC flattening or MbFC migration (Figure 6E), confirming JAK/STAT signaling specifically downregulates Br in SCs for proper flattening. The SCs lacking JAK/STAT accumulated less often in clusters when Br was concomitantly knocked down (Figure 6F), suggesting JAK/STAT signaling maintains proper SC dispersion through downregulation of Br. Statistical quantification and analysis through measuring the Average Number of Clustered Cells (see methods) further confirmed that loss-of-JAK/STAT activity has a higher average cell number in the cell clusters. Downregulation of Br in these JAK/STAT-knockdown cells could reduce the number of SCs in cell clusters (Figure 6G, 6H).

In addition, JAK/STAT activity reporter 10XSTAT-GFP was highly elevated in *br* mutant MbFCs, while it was undetectable in wild-type MbFCs (Figure 7A). Consistently, knockdown of Br in SCs enhanced 10XSTAT-GFP levels measured by signaling intensity (Figure 7B), indicating Br feeds back to suppress JAK/STAT activity in SCs. In this case, Br and JAK/STAT also mutually suppress each other's expression. Strong Br dominates in the MbFCs, while strong JAK/STAT signaling suppresses Br in SCs.

Gene expression shifts during the cuboidal-to-squamous transition.

Our genetic experiments revealed that ecdysone and JAK/STAT signaling suppressed Br for proper cuboidal-to-squamous transition. To begin to identify the collective shifts in gene expression which accompany the loss of Br during SC stretching, we turned to single-cell RNA sequencing techniques. In a recent Deng lab publication, we constructed a single-cell atlas of adult *Drosophila* ovary (Jevitt et al., 2020). This ovarian atlas sampled follicle cells in the process of undergoing the cuboidal-to-squamous transition but an in-depth analysis of their expression patterns during this transition was beyond the scope of establishing the atlas. To take a closer look at the expression patterns of the stretched cells, we re-analyzed these existing sequencing data using an updated version of the R package Seruat (version 4.0) which resulted in a Uniform Manifold Approximation and Projection (UMAP) plot containing 14 cell clusters (Figure 8A). We then used previously characterized marker gene expression to identify the cell-type identity of each cluster as in Jevitt et al., 2020 (Supplemental Figure 1). To focus on just the follicle cells of interest undergoing the cuboidal-to-squamous transition, we created a data subset which included the “Transitional FCs (Stg. 6–7)” and the “Stretched Cells” (Figure 8B). Using this subset, we could then ask which genes are more highly expressed in the SCs compared to the Transitional FCs by performing a differential expression analysis between the two clusters. Through this analysis, we identified 838 significantly differentially expressed genes; 224 genes were downregulated and 614 genes were upregulated in SCs (Supplemental Table 1).

We performed a functional enrichment analysis on the list of upregulated SC genes and identified that 326 Biological Process Gene Ontology (GO) terms were over-represented (Supplemental Table 2). Since many of these terms are related as parent and child in the GO hierarchy, we have chosen to highlight the 65 terms which are at the lowest level of the gene ontology hierarchy and thus are the most specific (Supplemental Table 2, Supplemental Figure 2). We have grouped these terms by their shared parent GO term (Supplemental Figure 2). Within this list we found six GO terms involved in anatomical structure morphogenesis; dorsal closure (GO:0007391), imaginal disc morphogenesis (GO:0007560), head involution (GO:0008258), imaginal disc-derived appendage morphogenesis (GO:0035114), post-embryonic appendage morphogenesis (GO:0035120), and establishment of ommatidial planar polarity (GO:0042067). We also found the term developmental growth involved in morphogenesis (GO:0060560) from the developmental process genes is present. During morphogenesis, individual cells must alter their shapes and this can occur through a number of different mechanisms including remodeling of the cytoskeleton, junctions, and extracellular matrix and we see GO terms relating to all of these cellular components. GO terms like regulation of cell shape (GO:0008360), extracellular matrix organization (GO:0030198), cell-cell junction assembly (GO:0007043), actin filament capping (GO:0051693), establishment or maintenance of cytoskeleton polarity (GO:0030952), and cortical actin cytoskeleton organization (GO: 0030866) are over-represented.

Since our interest is in which cell-shape-related genes are upregulated in the SCs, we identified the individual genes involved in contributing to cell shape and have highlighted their expression patterns between the Transitional FCs and SCs (Figure 8C). These

genes have been color coded to highlight their function in contributing to focal adhesion (GO:0005925), apical junction complex (GO:0043296), gap junction (GO:0005921), and cytoskeleton (GO:0005856). Interestingly, we found that collagen trimer (GO:0005581) genes involved in regulating collagen, a component of the basement membrane, were downregulated in SCs.

In addition, consistent with our experimental findings, we identified that many commonly-known ecdysone downstream targets, including *Hsp27* (Koelle et al., 1991), *ImpL2, tai* (Xie et al., 2015), *Hr4* (Gauhar et al., 2009), *ftz-f1* (Knapp et al., 2020), *Sox14* (Beckstead et al., 2005), *mys* (Kozlova and Thummel, 2003), *Diap1* (Lee et al., 2019), and *Pax* (Chen et al., 2008) are highly expressed in the SCs, further supporting the importance of ecdysone signaling in regulating the SC morphogenetic transition (Supplemental Table 1). We have also highlighted the expression patterns of transcription factors which are upregulated in SCs including the ecdysone targets *Sox14* and *ftz-f1* (Figure 8D). Consistent with our prior findings, Br is significantly downregulated in SCs (Supplemental Table 1). We also found a previously known JAK/STAT downstream target *apontic* (*apt*) (Starz-Gaiano et al., 2009), which is differentially upregulated during the cuboidal-to-squamous transition (Supplemental Table 1).

Discussion

Br is upregulated by Notch signaling around stage 5 during *Drosophila* oogenesis (Jia et al., 2014; Rowe et al., 2020), and here we report that the uniform pattern of Br in the follicular epithelium is gradually lost in the anterior follicle cells (SCs and BCs) from stage 9 to 10a. This downregulation of Br appears functionally significant, as misexpression of Br-Z1 in the SCs blocks their proper cuboidal-to-squamous transition. The ecdysone and JAK/STAT pathways have been implicated in BC migrations, ecdysone regulates the timing of BC movement, and the JAK/STAT pathway mobilizes the BCs (Montell et al., 2012). Here, we show that the strong upregulation of ecdysone and JAK/STAT signaling in the anterior follicle cell subset SCs mediates the downregulation of Br. The activities of both pathways are high in the anterior follicle cells from stage 8. Their strong upregulation mutually antagonizes the downregulated expression pattern of Br. Suppression of either signaling pathway leads to flattening defects and Br upregulation. Knockdown of *br* in either ecdysone- or JAK/STAT-defective SCs alleviates the severity of stretching and dispersion defects, suggesting the importance of Br suppression for morphological remodeling of SC.

Our results and those of others (Jang et al., 2009) confirmed a pulse of ecdysone activity at stages 8/9. Given the ability of Br to feed back into JAK/STAT and ecdysone, we propose that this pulse of ecdysone activity at stages 8/9 leads to downregulation of Br in SCs, which in turn further de-represses ecdysone activity, leading to a feedback loop to continuously upregulate ecdysone activity and downregulate Br. Meanwhile, downregulated Br might also de-repress JAK/STAT activity, which again further suppresses Br. In summary, ecdysone and JAK/STAT synergize to suppress Br in order to further de-repress themselves for proper cuboidal-to-squamous transition. Taken together with our previously published results that Br is upregulated by Notch after stage 5 (Jia et al., 2014), we currently propose Br expression is sensitive to the Notch, ecdysone and JAK/STAT pathways, serving as an

important spatiotemporal cue for proper cell differentiation, movement and morphological changes in SCs (Figure 9). While strong ecdysone and JAK/STAT signaling suppresses Br in SCs, strong Br dominates in the MbFCs. We showed *br* mutant clones in the MbFCs expressed highly elevated JAK/STAT activity reporter 10XSTAT-GFP. What signal activates JAK/STAT? Could Upd reach far toward the posterior of egg chamber? Or can polar cells from the adjacent egg chamber send the signal at an earlier stage of development? Our Figure 7A egg chamber is at stage 10A, which should have severed the connection with the adjacent egg chamber at an earlier stage of development. However, we can't rule out the possibility of residual effects caused by previous connection with polar cells of the adjacent egg chamber. To further confirm whether a downregulation of Br happens in MbFCs by activating JAK/STAT, we made flip-out clones to activate Upd and Stat92E. We found that activation of neither Upd nor constitutive active Stat92E could downregulate Br in MbFCs (Supplemental Figure 3). During *Drosophila* oogenesis, different subpopulations of follicle cells undergo distinct differentiation under the influence of multiple signaling pathways. For instance, MbFCs first receive Notch signaling to undergo the mitotic cycle-endocycle switch at stages 5/6. In addition to Notch signaling during the endocycle, the EGFR pathway acts together with JAK/STAT to induce posterior follicle cell fate of MbFCs at the posterior of the egg chamber. Later upregulation of EcR and Ttk69 switches the cell cycle program from endocycle to gene amplification in the chorion gene loci of MbFCs (Klusza and Deng, 2011). The multiple signaling influences and complex signaling networks might cause the different responses that neither expressing Upd or activating Stat92E in MbFCs downregulated Br.

Ecdysone signaling is required for initiation of SC stretching

Close examinations suggest Br should not be the only factor acting downstream of ecdysone. Overexpression of Br caused flattening defects of SCs, but SCs are evenly dispersed on the surface areas of the anterior follicular epithelium (Figure 2C), while the repressed ecdysone signaling largely resulted in severe SCs accumulation at the anterior terminus of egg chamber (Figure 3D), whereas co-suppression of Br and ecdysone only partially alleviated the accumulation of SCs at the anterior (Figure 3F, 3H). These results suggest the main role of ecdysone signaling is to initiate the mobility of SCs to stretch, and that suppression of Br partially contributes to this initiation process. We have identified a number of potential downstream targets of Br which are complementary to its expression using the single-cell RNA sequencing data. Consistent with our hypothesis, we identified that many other ecdysone downstream targets from the single-cell RNA sequencing data, which are differentially expressed in the SCs. These ecdysone downstream targets include *Hsp27*, *ImpL2*, *tai*, *Hr4*, *ftz-f1*, *Sox14*, *mys*, *Diap*, and *Pax* (Supplemental Table 1).

JAK/STAT signaling is required for SC dispersion and cell fate determination

JAK/STAT signaling affects the dispersion of SCs, though its effect is weak during the regulation of morphogenetic movement of SCs. In our report, knockdown of JAK/STAT in post-mitotic SCs weakly upregulates Br expression (Figure 6D), while knockdown of JAK/STAT in mitotic SCs has a robust Br upregulation and severe SC clustering (Figure 6C). These findings indicate effects of JAK/STAT during mitosis might significantly contribute to the dispersion of SCs. JAK/STAT signaling is restricted to polar cells before the mitotic

cycle/endocycle (M/E) switch, and it does not affect the M/E switch transition (Assa-Kunik et al., 2007), suggesting that loss of JAK/STAT does not keep SCs in an undifferentiated cell fate. In addition, follicle cells with undifferentiated cell fates actually lack Br expression (Jia et al., 2014). In our study, JAK/STAT-knockdown SCs retain high levels of Br and display SC clustering, which resembles MbFCs. These findings are consistent with a previous report that JAK/STAT is important for anterior cell fate determination (Xi et al., 2003). In summary, JAK/STAT determines anterior cell fate in the mitotic cycle, together with this early effect, the post-mitotic effect of JAK/STAT in SCs further contributes to the SC dispersal. Interestingly, we also found a previously known JAK/STAT downstream target *apt* to be differentially upregulated during the cuboidal-to-squamous transition (Supplemental Table 1). Previous studies have identified that APT is a feedback regulator of the JAK/STAT pathway. A graded signal molecule Unpaired (UPD) emerges from the anterior follicle cells to activate the JAK/STAT pathway, STAT then locally activates APT, its own repressor, to have a negative feedback. When JAK/STAT signaling is highly expressed, it activates Slow Border Cells (SLBO) as well, which can inhibit the APT feedback repression. In this case, the border cells (BCs) are nice examples. BCs have high levels of JAK/STAT and SLBO, and eventually migrate out of the anterior epithelial cell layer. When JAK/STAT signaling is lower, with more APT than SLBO, the cells will eventually lose JAK/STAT activity, and stay in the follicular epithelium (Starz-Gaiano et al., 2009). In our results, APT is highly expressed in the SCs, while SLBO is not. It perfectly explains that JAK/STAT is a transient signaling, its pulsative activation might only briefly influence Br at the beginning of stage 8. In consistent with it, our experimental results showed JAK/STAT signaling actually goes down from stage 8 to stage 10 in SCs, and its activity is significantly lower than BCs (Figure 6A,6B).

Mechanistic understanding of SC flattening defects.

Throughout early oogenesis, follicle cells maintain a cuboidal shape, interconnected with adherens junctions made up of adhesion proteins like E-Cadherin (E-cad) and Armadillo (Arm, also known as β-catenin in humans). Later, in midoogenesis, SCs start to transition from cuboidal to squamous in shape. During this cell shape remodeling, E-cad and Arm gradually decrease, and disappear at stage 10a (Grammont, 2007; Melani et al., 2008), similar to the Br expression pattern. The dynamics of adherens junction remodeling has been known to control SC flattening, and downregulation of E-cad and Arm is responsible for the reduced SC density in the anterior half of egg chamber (Grammont, 2007; Melani et al., 2008). In addition, E-cad and Arm are interchangeable as markers for adherens junctions (Melani et al., 2008). We focused on Arm to ascertain the adhesion status of the defective SCs.

In EcR-B1-repressed SCs, where stretching defects were more extreme, Arm was highly accumulated and the SC layer was seemingly less compliant. This resulted in large tears in the epithelium (Figure 4). This EcR-B1 knockdown stretching defect was distinct from that of br-Z1 overexpression. Overexpression of br-Z1 resulted in a lack of stretching with a very low level of Arm and no apparent tearing of the epithelial layer. These results are consistent with the idea that SC flattening is a response to growth of the germline and is reliant on SC compliance (Kolahi et al., 2009). Establishing the proper level of

compliance in SCs may be controlled by EcR-B1 through suppression of Arm which would reduce the number of adherens junctions thereby reducing the rigidity of the SC layer. We proposed that ecdysone and JAK/STAT synergize to suppress Br in order to further de-repress themselves for proper cuboidal-to-squamous transition. There are still many unknowns regarding to the molecular mechanisms underlying this transition. For instance, this study is the first to reveal an inhibitory role of ecdysone signaling in suppressing Br for SC stretching. Br has been known to be a positively regulated target by ecdysone, therefore there could be another possibility that ecdysone might activate a Br repressor, and indirectly downregulate Br. To explore the molecular mechanisms, we further performed a differential expression analysis, which identified 838 significantly differentially expressed genes; 224 genes were downregulated and 614 genes were upregulated in SCs (Supplemental Table 1). We performed a GO analysis and included the full results in the Supplemental Table 2. We also included the Supplemental Figure 2 highlighting the morphogenesis, cell-shape change related, as well as other GO terms, which were overrepresented in the SCs. This result further reinforced that biological processes involved in morphogenesis were indeed statistically over-represented in this SC cluster compared to the transitional FC cluster. Additionally, genes that were upregulated in SCs were also involved in other morphogenetic events such as tube development and neuron development. These are interesting new insights. Further analysis of these genes potentially gives us a better understanding of participants involved in regulating SC morphological functions.

Materials and Methods

Fly Strains and Genetics

The following fly Strains were used: $br^{npr\text{-}3}$ (amorphic allele) (Jia et al., 2014; Kiss et al., 1980), *UAS-br-Z1* (Zhou and Riddiford, 2002), *UAS-br RNAi* (Bloomington *Drosophila* Stock Center, BDSC#27272), *EcRE-lacZ* (BDSC#4516), *UAS-EcR-B1 W650A* (BDSC#6872), *10XSTAT92E-GFP* (BDSC#26197), *UAS-Stat92E RNAi* (BDSC#33637), *UAS-dome RNAi* (Vienna *Drosophila* Resource Center, VDRC #106071), *A90-Gal4, UAS-mRFP* (Tran and Berg, 2003), *B42-lacZ* (kindly provided by Trudi Schüpbach), *UAS-Upd* (Harrison et al., 1998) (kindly provided by Norbert Perrimon), $UAS\text{-}Stat92E^{CA}$ (Ekas et al., 2010) (kindly provided by Erika Bach), *patched (ptc)-GAL4*, *UAS-GFP* (Tamori and Deng, 2013), and w^{1118} as a wild-type control.

For FLP/FRT clone induction (Golic and Lindquist, 1989; Xu and Rubin, 1993), previously described procedures were followed (Sun and Deng, 2005). To generate mosaic egg chambers expressing UAS constructs, the flip-out Gal4 (Pignoni and Zipursky, 1997) stock *hsFLP;actin<CD2<Gal4,UAS-RFP/TM3,Sb* was applied. Flip-out clones were induced by 30 minute heat shock at 37°C and fed with yeast for two days before dissection. The temporal and regional gene expression targeting (TARGET) technique was applied to control spatiotemporal gene expression (McGuire et al., 2004). Flies were raised at 18°C until adulthood, then shifted to 29°C for 48h before dissection.

Immunohistochemistry and Image Analysis

Immunohistochemistry and image acquisition were performed as previously described (Jia et al., 2015; Sun and Deng, 2005). The following antibodies were used: mouse anti-Br-Core (25E9) 1:30, mouse anti-Arm (N2 7A1) 1:40 (Development Studies Hybridoma Bank, USA), rabbit anti-β-Galactosidase 1:5000 (Sigma, USA). Corresponding Alexa Fluor secondary antibodies (1:400; Invitrogen) were selected according to primary antibodies. Images were acquired with Zeiss confocal microscopes (LSM 510 at Florida State University, LSM 700 at Georgia Southern University, LSM 800 at Tulane University) and processed in Photoshop and Image J. Signal intensity was measured by the Interactive 3D Surface Plot Plugin of Image J. To generate line profiles, images were opened in Image J, a 12 μm line was drawn perpendicular to the stretched cell layer using the straight line tool, and the Intensity Profile tool was used to plot the profile.

Statistical Quantification and Analysis

In order to measure the accumulation of SCs, we calculated the Accumulation Percentage (AP). AP=(a/b)*100% (Figure 3H); a as the width of clustered cells (distance between the anterior terminus and the posterior end), b as the width of the anterior half of the egg chamber. In order the count the Average Number of Clustered Cells (ANCC), we calculated the number of clustered cells in the anterior half of the egg chamber, excluding the anterior-most termini. ANCC=(X+ Y+Z)/3 (Figure 6H); X, Y, Z are the numbers of the top three most abundant clustered cells within one cell diameter distance. The statistical analyses were performed using GraphPad Prism (version 6.0; GraphPad Software). Data were expressed as the mean ± SEM. Intergroup differences were assessed by Student's t-test. Statistical significance is denoted with asterisks in the figures.

Single-Cell RNA Sequencing Analysis

Our wild-type ovary single-cell RNA sequencing dataset is currently publicly available (GEO accession #GSE146040), and was used as in a previous work (Jevitt et al., 2020). We re-analyzed the data focusing on the cuboidal-to-squamous transition. All analyses were done using Seurat version 4.0 (Stuart et al., 2019). The entire dataset containing 14 clusters were identified using Subset data with just transitional FCs and SCs was made using the Seurat function subset. Differential expression analysis was performed using the Seurat function FindMarkers with ident.1 = SCs and ident.2 = transitional FCs. Heatmaps were generated for markers of interest with the DoHeatmap function. In addition, the R script used for sequencing analysis in this work can be found at https://github.com/ajevitt3/ScRNA-sequencing-analysis-stretched-cells.git.

Supplementary Material

Refer to Web version on PubMed Central for supplementary material.

Acknowledgments and Research Funding

We would like to thank the Biological Science Imaging Facility at Florida State University, Georgia Southern University and Tulane University for technical help. Dr. Douglas Harrison, The DSHB, the TRiP at Harvard Medical School (NIH/NIGMS R01-GM084947), Vienna *Drosophila* Resource Center and the Bloomington

Drosophila Stock Center for providing us antibodies and fly stocks. Special thanks to Yoichiro Tamori, Gabriel Calvin and other members of the Deng lab for technical help and discussions on this project. D.J. was supported by Dissertation Research Grant Award from Florida State University and Faculty Research Committee (FRC) Award and COSM Research Grant Award from Georgia Southern University; B.R. is supported by McNair Scholarship, Chandler Scholarship and Undergraduate Student Research Assistantship from Georgia Southern University; W.-M. D. is supported by the National Institute of Health grant (R01GM072562) and National Science Foundation (IOS-1052333).

References

Assa-Kunik E, Torres IL, Schejter ED, Johnston DS, Shilo BZ, 2007. Drosophila follicle cells are patterned by multiple levels of Notch signaling and antagonism between the Notch and JAK/STAT pathways. Development 134, 1161–1169. [PubMed: 17332535]

Bach EA, Ekas LA, Ayala-Camargo A, Flaherty MS, Lee H, Perrimon N, Baeg GH, 2007. GFP reporters detect the activation of the Drosophila JAK/STAT pathway in vivo. Gene Expr Patterns 7, 323–331. [PubMed: 17008134]

Besse F, Pret AM, 2003. Apoptosis-mediated cell death within the ovarian polar cell lineage of Drosophila melanogaster. Development 130, 1017–1027. [PubMed: 12538526]

Boyle MJ, Berg CA, 2009. Control in time and space: Tramtrack69 cooperates with Notch and Ecdysone to repress ectopic fate and shape changes during Drosophila egg chamber maturation. Development 136, 4187–4197. [PubMed: 19934014]

Brigaud I, Duteyrat JL, Chlasta J, Le Bail S, Couderc JL, Grammont M, 2015. Transforming Growth Factor beta/activin signalling induces epithelial cell flattening during Drosophila oogenesis. Biology open 4, 345–354. [PubMed: 25681395]

Brown HL, Cherbas L, Cherbas P, Truman JW, 2006. Use of time-lapse imaging and dominant negative receptors to dissect the steroid receptor control of neuronal remodeling in Drosophila. Development 133, 275–285. [PubMed: 16354717]

Buszczak M, Freeman MR, Carlson JR, Bender M, Cooley L, Segraves WA, 1999. Ecdysone response genes govern egg chamber development during mid-oogenesis in Drosophila. Development 126, 4581–4589. [PubMed: 10498692]

Cetera M, Ramirez-San Juan GR, Oakes PW, Lewellyn L, Fairchild MJ, Tanentzapf G, Gardel ML, Horne-Badovinac S, 2014. Epithelial rotation promotes the global alignment of contractile actin bundles during Drosophila egg chamber elongation. Nat Commun 5, 5511. [PubMed: 25413675]

Cherbas L, Hu X, Zhimulev I, Belyaeva E, Cherbas P, 2003. EcR isoforms in Drosophila: testing tissue-specific requirements by targeted blockade and rescue. Development 130, 271–284. [PubMed: 12466195]

Deng WM, Althauser C, Ruohola-Baker H, 2001. Notch-Delta signaling induces a transition from mitotic cell cycle to endocycle in Drosophila follicle cells. Development 128, 4737–4746. [PubMed: 11731454]

Ekas LA, Cardozo TJ, Flaherty MS, McMillan EA, Gonsalves FC, Bach EA, 2010. Characterization of a dominant-active STAT that promotes tumorigenesis in Drosophila. Dev Biol 344, 621–636. [PubMed: 20501334]

Emery IF, Bedian V, Guild GM, 1994. Differential expression of Broad-Complex transcription factors may forecast tissue-specific developmental fates during Drosophila metamorphosis. Development 120, 3275–3287. [PubMed: 7720567]

Gauhar Z, Sun LV, Hua S, Mason CE, Fuchs F, Li TR, Boutros M, White KP, 2009. Genomic mapping of binding regions for the Ecdysone receptor protein complex. Genome Res 19, 1006–1013. [PubMed: 19237466]

Ghiglione C, Devergne O, Cerezo D, Noselli S, 2008. Drosophila RalA is essential for the maintenance of Jak/Stat signalling in ovarian follicles. EMBO reports 9, 676–682. [PubMed: 18552769]

Golic KG, Lindquist S, 1989. The FLP recombinase of yeast catalyzes site-specific recombination in the Drosophila genome. Cell 59, 499–509. [PubMed: 2509077]

Gomez JM, Wang Y, Riechmann V, 2012. Tao controls epithelial morphogenesis by promoting Fasciclin 2 endocytosis. The Journal of cell biology 199, 1131–1143. [PubMed: 23266957]

Grammont M, 2007. Adherens junction remodeling by the Notch pathway in Drosophila melanogaster oogenesis. The Journal of cell biology 177, 139–150. [PubMed: 17420294]

Haigo SL, Bilder D, 2011. Global tissue revolutions in a morphogenetic movement controlling elongation. Science 331, 1071–1074. [PubMed: 21212324]

Harrison DA, McCoon PE, Binari R, Gilman M, Perrimon N, 1998. Drosophila unpaired encodes a secreted protein that activates the JAK signaling pathway. Genes Dev 12, 3252–3263. [PubMed: 9784499]

Hu X, Cherbas L, Cherbas P, 2003. Transcription activation by the ecdysone receptor (EcR/USP): identification of activation functions. Molecular endocrinology 17, 716–731. [PubMed: 12554759]

Jang AC, Chang YC, Bai J, Montell D, 2009. Border-cell migration requires integration of spatial and temporal signals by the BTB protein Abrupt. Nature cell biology 11, 569–579. [PubMed: 19350016]

Jevitt A, Chatterjee D, Xie G, Wang XF, Otwell T, Huang YC, Deng WM, 2020. A single-cell atlas of adult Drosophila ovary identifies transcriptional programs and somatic cell lineage regulating oogenesis. PLoS Biol 18, e3000538. [PubMed: 32339165]

Jia D, Huang YC, Deng WM, 2015. Analysis of Cell Cycle Switches in Drosophila Oogenesis. Methods in molecular biology 1328, 207–216. [PubMed: 26324440]

Jia D, Tamori Y, Pyrowolakis G, Deng WM, 2014. Regulation of broad by the Notch pathway affects timing of follicle cell development. Developmental biology 392, 52–61. [PubMed: 24815210]

Jia D, Xu Q, Xie Q, Mio W, Deng WM, 2016. Automatic stage identification of Drosophila egg chamber based on DAPI images. Scientific reports 6, 18850. [PubMed: 26732176]

Karim FD, Guild GM, Thummel CS, 1993. The Drosophila Broad-Complex plays a key role in controlling ecdysone-regulated gene expression at the onset of metamorphosis. Development 118, 977–988. [PubMed: 8076529]

Keller R, Davidson LA, Shook DR, 2003. How we are shaped: the biomechanics of gastrulation. Differentiation; research in biological diversity 71, 171–205. [PubMed: 12694202]

Kerridge S, Munjal A, Philippe JM, Jha A, de las Bayonas AG, Saurin AJ, Lecuit T, 2016. Modular activation of Rho1 by GPCR signalling imparts polarized myosin II activation during morphogenesis. Nat Cell Biol 18, 261–270. [PubMed: 26780298]

Kiss I, Szabad J, Belyaeva ES, Zhimulev IF, Major J, 1980. Genetic and developmental analysis of mutants in an early ecdysone-inducible puffing region in Drosophila melanogaster. Basic life sciences 16, 163–181. [PubMed: 6779790]

Klusza S, Deng WM, 2011. At the crossroads of differentiation and proliferation: precise control of cell-cycle changes by multiple signaling pathways in Drosophila follicle cells. Bioessays 33, 124–134. [PubMed: 21154780]

Koelle MR, Talbot WS, Segraves WA, Bender MT, Cherbas P, Hogness DS, 1991. The Drosophila EcR gene encodes an ecdysone receptor, a new member of the steroid receptor superfamily. Cell 67, 59–77. [PubMed: 1913820]

Kolahi KS, White PF, Shreter DM, Classen AK, Bilder D, Mofrad MR, 2009. Quantitative analysis of epithelial morphogenesis in Drosophila oogenesis: New insights based on morphometric analysis and mechanical modeling. Developmental biology 331, 129–139. [PubMed: 19409378]

Kozlova T, Thummel CS, 2003. Essential roles for ecdysone signaling during Drosophila mid-embryonic development. Science 301, 1911–1914. [PubMed: 12958367]

Mateo M, Generous A, Sinn PL, Cattaneo R, 2015. Connections matter--how viruses use cell-cell adhesion components. Journal of cell science 128, 431–439. [PubMed: 26046138]

McGuire SE, Mao Z, Davis RL, 2004. Spatiotemporal gene expression targeting with the TARGET and gene-switch systems in Drosophila. Science's STKE : signal transduction knowledge environment 2004, pl6.

Melani M, Simpson KJ, Brugge JS, Montell D, 2008. Regulation of cell adhesion and collective cell migration by hindsight and its human homolog RREB1. Curr Biol 18, 532–537. [PubMed: 18394891]

Miao H, Blankenship JT, 2020. The pulse of morphogenesis: actomyosin dynamics and regulation in epithelia. Development 147.

Montell DJ, Yoon WH, Starz-Gaiano M, 2012. Group choreography: mechanisms orchestrating the collective movement of border cells. Nat Rev Mol Cell Biol 13, 631–645. [PubMed: 23000794]

Mugat B, Brodu V, Kejzlarova-Lepesant J, Antoniewski C, Bayer CA, Fristrom JW, Lepesant JA, 2000. Dynamic expression of broad-complex isoforms mediates temporal control of an ecdysteroid target gene at the onset of Drosophila metamorphosis. Dev Biol 227, 104–117. [PubMed: 11076680]

Nilson LA, Schupbach T, 1999. EGF receptor signaling in Drosophila oogenesis. Current topics in developmental biology 44, 203–243. [PubMed: 9891881]

Osterfield M, Schupbach T, Wieschaus E, Shvartsman SY, 2015. Diversity of epithelial morphogenesis during eggshell formation in drosophilids. Development 142, 1971–1977. [PubMed: 25953345]

Peters NC, Berg CA, 2016. Dynamin-mediated endocytosis is required for tube closure, cell intercalation, and biased apical expansion during epithelial tubulogenesis in the Drosophila ovary. Developmental biology 409, 39–54. [PubMed: 26542010]

Pignoni F, Zipursky SL, 1997. Induction of Drosophila eye development by decapentaplegic. Development 124, 271–278. [PubMed: 9053304]

Roth S, Lynch JA, 2009. Symmetry breaking during Drosophila oogenesis. Cold Spring Harbor perspectives in biology 1, a001891. [PubMed: 20066085]

Rowe M, Paculis L, Tapia F, Xu Q, Xie Q, Liu M, Jevitt A, Jia D, 2020. Analysis of the Temporal Patterning of Notch Downstream Targets during Drosophila melanogaster Egg Chamber Development. Sci Rep 10, 7370. [PubMed: 32355165]

Schock F, Perrimon N, 2002. Cellular processes associated with germ band retraction in Drosophila. Developmental biology 248, 29–39. [PubMed: 12142018]

Schubiger M, Carre C, Antoniewski C, Truman JW, 2005. Ligand-dependent de-repression via EcR/USP acts as a gate to coordinate the differentiation of sensory neurons in the Drosophila wing. Development 132, 5239–5248. [PubMed: 16267093]

Shyu LF, Sun J, Chung HM, Huang YC, Deng WM, 2009. Notch signaling and developmental cell-cycle arrest in Drosophila polar follicle cells. Mol Biol Cell 20, 5064–5073. [PubMed: 19846665]

Spradling A, 1993. Developmental genetics of oogenesis in The development of *Drosophila* melanogaster. CSHL Press, 1–70.

Starz-Gaiano M, Melani M, Meinhardt H, Montell D, 2009. Interpretation of the UPD/JAK/STAT morphogen gradient in Drosophila follicle cells. Cell Cycle 8, 2917–2925. [PubMed: 19729999]

Sun J, Deng WM, 2005. Notch-dependent downregulation of the homeodomain gene cut is required for the mitotic cycle/endocycle switch and cell differentiation in Drosophila follicle cells. Development 132, 4299–4308. [PubMed: 16141223]

Tamori Y, Deng WM, 2013. Tissue repair through cell competition and compensatory cellular hypertrophy in postmitotic epithelia. Dev Cell 25, 350–363. [PubMed: 23685249]

Thummel CS, 1996. Flies on steroids--Drosophila metamorphosis and the mechanisms of steroid hormone action. Trends Genet 12, 306–310. [PubMed: 8783940]

Tian AG, Tamori Y, Huang YC, Melendez NT, Deng WM, 2013. Efficient EGFR signaling and dorsal-ventral axis patterning requires syntaxin dependent Gurken trafficking. Developmental biology 373, 349–358. [PubMed: 23127433]

Tran DH, Berg CA, 2003. bullwinkle and shark regulate dorsal-appendage morphogenesis in Drosophila oogenesis. Development 130, 6273–6282. [PubMed: 14602681]

Tzolovsky G, Deng WM, Schlitt T, Bownes M, 1999. The function of the broad-complex during Drosophila melanogaster oogenesis. Genetics 153, 1371–1383. [PubMed: 10545465]

Xi R, McGregor JR, Harrison DA, 2003. A gradient of JAK pathway activity patterns the anterior-posterior axis of the follicular epithelium. Developmental cell 4, 167–177. [PubMed: 12586061]

Xu T, Rubin GM, 1993. Analysis of genetic mosaics in developing and adult Drosophila tissues. Development 117, 1223–1237. [PubMed: 8404527]

Zhou X, Riddiford LM, 2002. Broad specifies pupal development and mediates the ‘status quo’ action of juvenile hormone on the pupal-adult transformation in Drosophila and Manduca. Development 129, 2259–2269. [PubMed: 11959833]

Highlights

- Notch, ecdysone and JAK/STAT signaling controls Broad to change the epithelial shape.
- Ecdysone signaling regulates follicle cell stretching and dispersion.
- JAK/STAT ensures proper spacing between cells to prevent clustering.
- Single-cell RNA sequencing data reveal genes expressed during cell shape change.

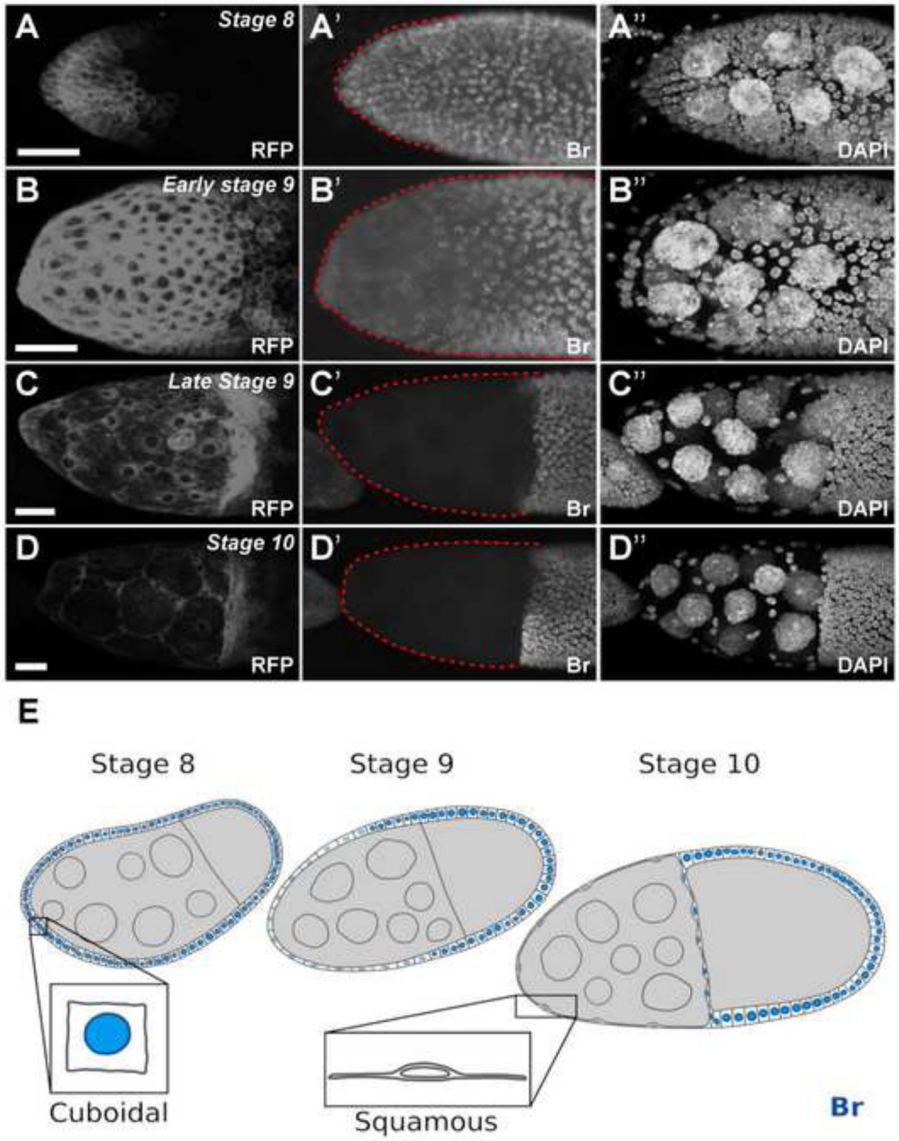

Figure 1.

The Br pattern in follicle cells during midoogensis. (A-D) SCs marked by RFP (A90-Gal4, UAS-mRFP) in white. (A') Br was expressed in all MbFCs at stage 8. (B') Br expression started to decrease in anterior follicle cells at stage 9, including SCs (surrounded by red dotted line). (C') Br expression was absent in SCs (surrounded by red dotted line) at by late stage 9 and remains absent in stage 10a (D') Br expression remains absent in SCs (surrounded by red dotted line) in stage 10a. (E) Illustration depicting that from stage 8 to stage 10a, SCs gradually flatten in shape, from cuboidal to squamous as Br expression is gradually reduced. DAPI staining marks cell nuclei. Anterior is to the left. Bars, 20 μm.

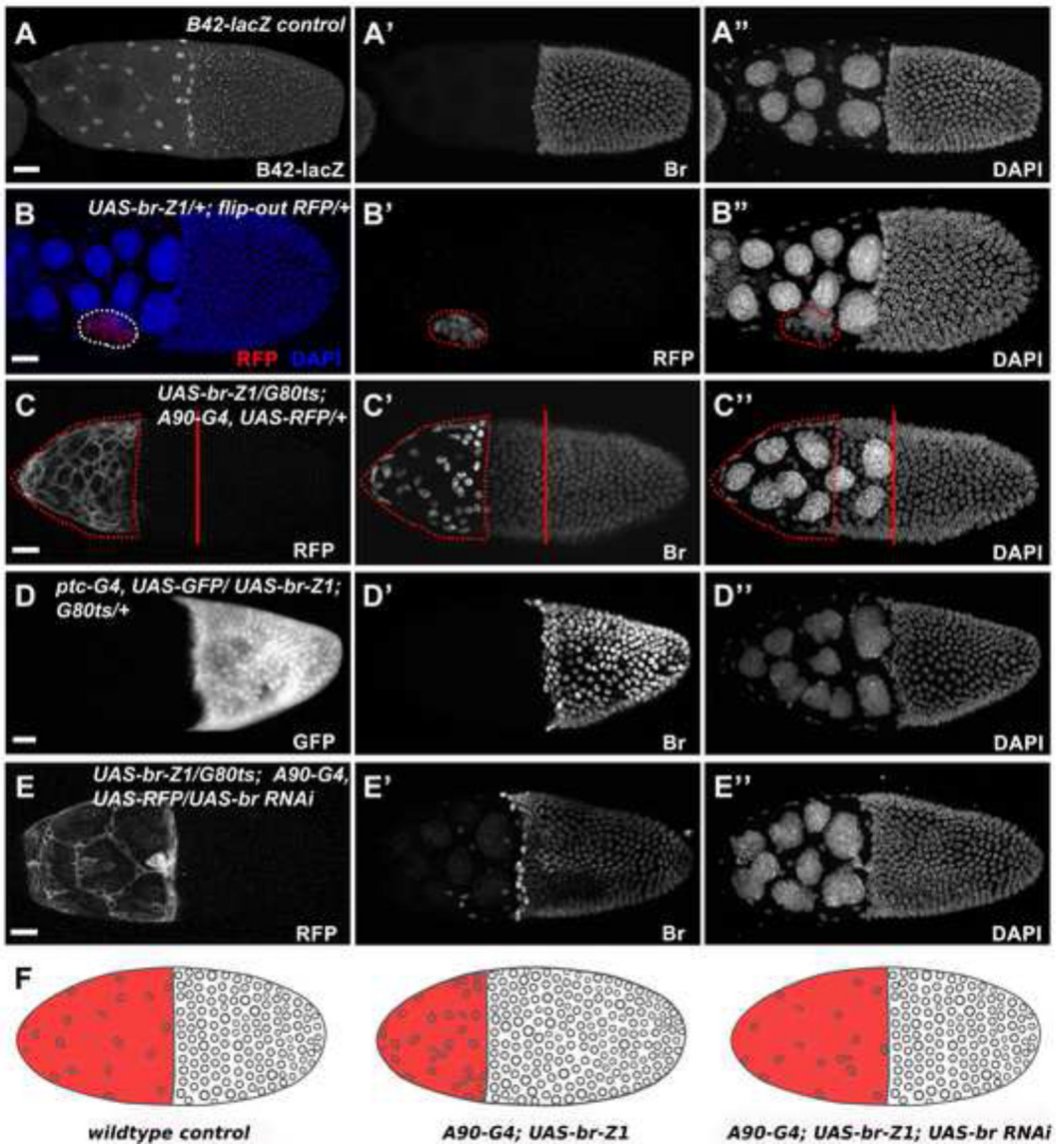

Figure 2.

Misexpression of Br in the SCs disrupts proper SC stretching. (A) Expression of enhancer trap line *B42-lacZ* (white in A) was applied to visualize proper SC flattening. (B) Br-Z1-misexpressing clones (red in B, white in B'; outlined) created by the flip-out Gal4/UAS technique caused failed SC flattening. (C) Br-Z1 misexpression (white in C; outlined) driven by SC-expressed A90-Gal4 caused failed SC flattening and slower MbFC migration. (D) Br-Z1 misexpression (white in D) driven by MbFC-specific ptc-Gal4 did not affect SC flattening and MbFC migration. (E) Introducing *br* RNAi in Br-Z1-misexpressing SCs (white in E) driven by A90-Gal4 restored proper SC flattening and MbFC migration. (F) Diagrams depict the accumulation of SCs in different genetic backgrounds. DAPI staining marks cell nuclei. Anterior is to the left. Bars, 20 μm.

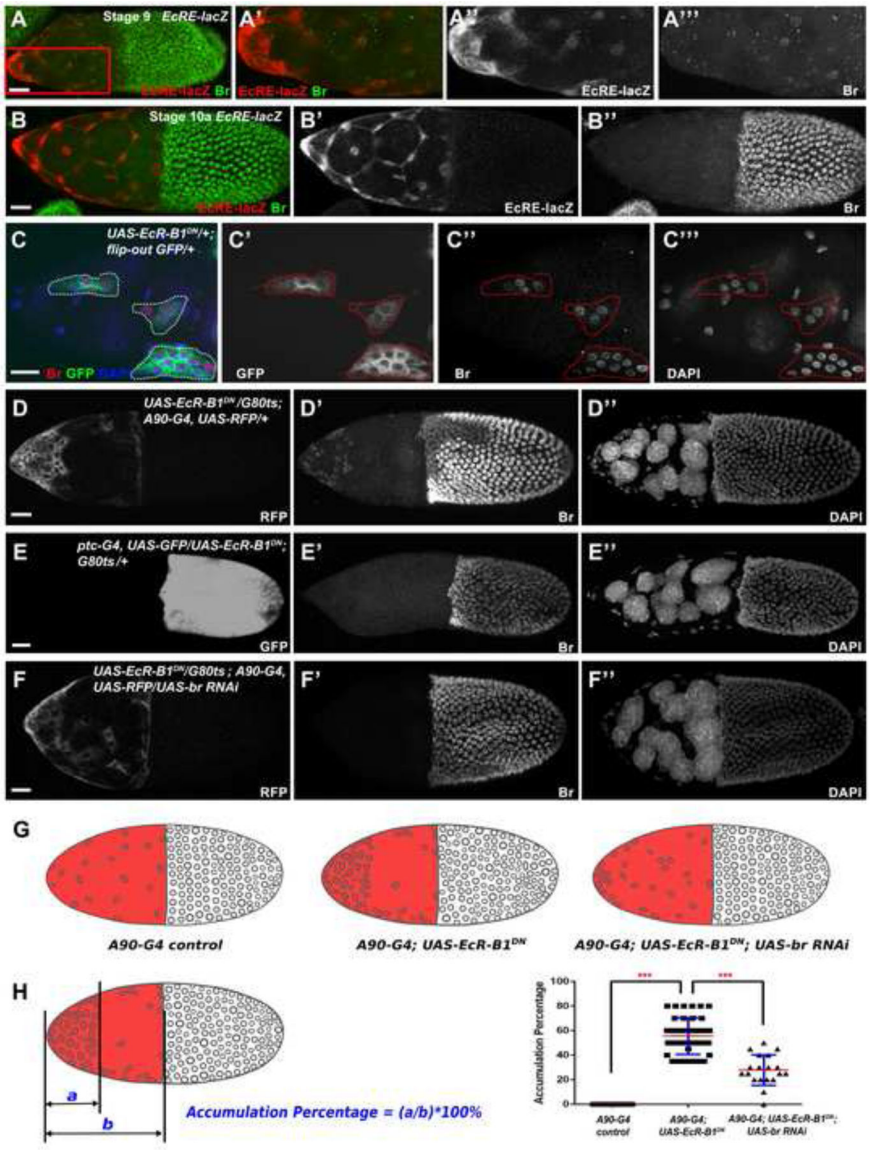

Figure 3.

Ecdysone signaling mediates downregulation of Br in the SCs. (A-B) Expression of ecdysone activity reporter *EcRE-lacZ* showed a pulse of ecdysone activity from stage 9 in the anterior cells, including SCs. The increased expression of *EcRE-lacZ* (red in A, A', white in A") is in contrast to decreased Br expression (green in A, A', white in A'"). Ecdysone activity peaks at stage 10a (red in B, white in B'), and no Br (green in B, white in B") was detected. (C) In EcR-B1 function repressed clones (green in C, white in C') created by the flip-out Gal4/UAS technique, SCs of a stage 10a egg chamber failed to flatten properly. (D) EcR repression driven by the SC-expressed A90-Gal4 (white in D) caused severe accumulation of SCs at the anterior. (E) Loss of EcR function in MbFCs (white in E) did not affect SC flattening and MbFC migration. (F) Introducing *br* RNAi in EcR-B1-repressed SCs partially restored proper SC flattening and MbFC migration. (G) Diagrams depict the accumulation of SCs in different genetic backgrounds. (H) The Accumulation

Percentage (AP) was applied to measure the accumulation of SCs. Statistical differences of AP were observed between *A90-Gal4* control (n=19) and *A90-Gal4; UAS-EcR-B1^{DN}* group (n=39), *A90-Gal4; UAS-EcR-B1^{DN}* and *A90-Gal4; UAS-EcR-B1^{DN}; UAS-br RNAi* group (n=19), respectively. ***p<0.001. DAPI staining marks cell nuclei. Anterior is to the left. Bars, 20 μm.

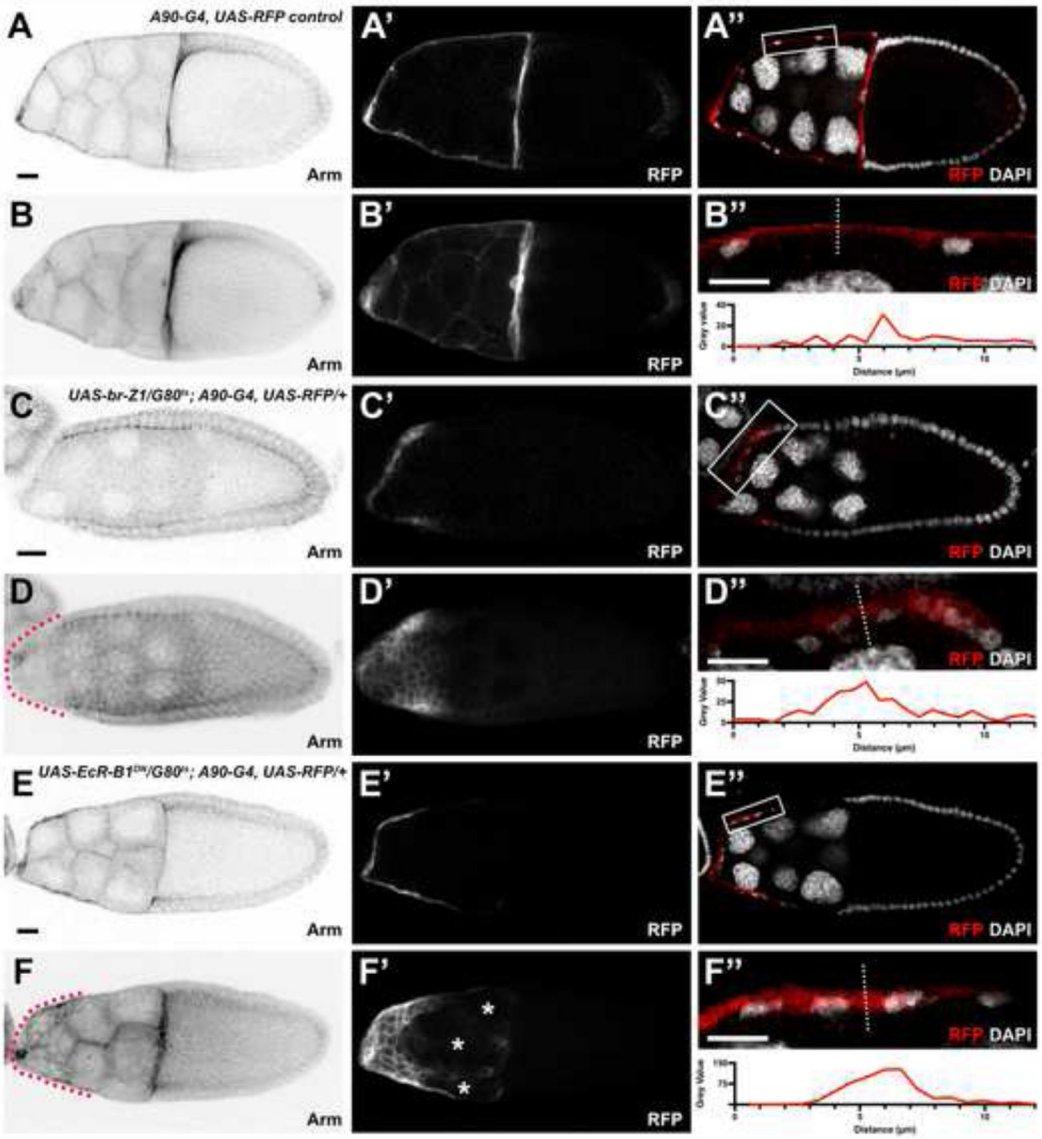

Figure 4.

Ecdysone signaling suppresses arm in the SCs. (A-F) Arm staining (black) for each genotype at stage 10 from images taken of the midsagittal plane (A, C, E) and projection (B, D, F). Red dotted lines outline the SCs. (A'-F') RFP driven by the SC-expressed A90-Gal4 (white). Asterisks mark holes in the SC layer. (A", C", E") RFP driven by the SC-expressed A90-Gal4 (red) with DAPI staining (white). White box marks region of interest (ROI) which is shown below each image. (B", D", F") ROI zoomed in to show SCs from the image above. White dotted line demonstrates where 12 μm line was drawn for the line profile shown below. Gray value is the intensity measurement of the A90-Gal4 driven RFP expression. DAPI staining marks cell nuclei. Anterior is to the left. Bars, 20 μm.

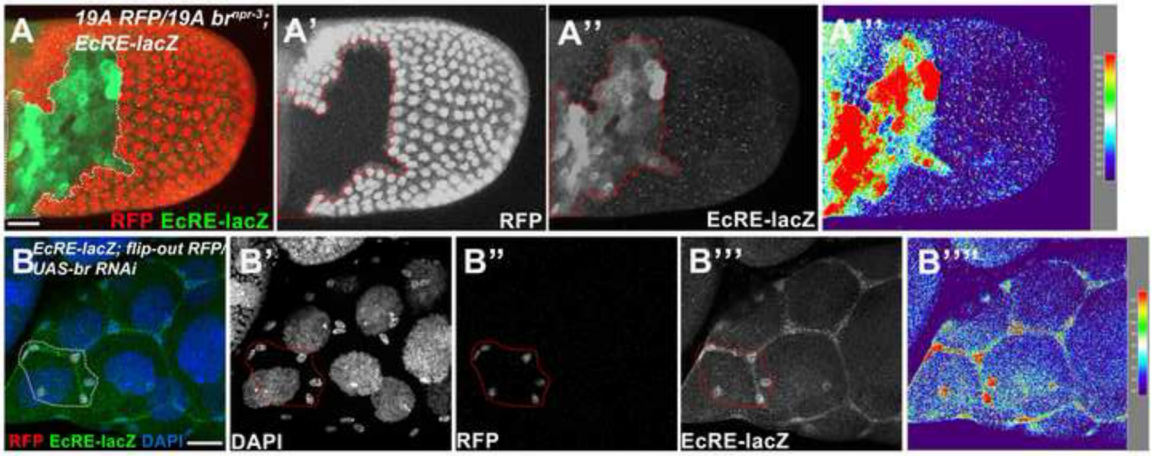

Figure 5.

Br feeds back to suppress ecdysone activity. (A) Stage 10a $br^{npr\text{-}3}$ follicle-cell clones (marked by the absence of RFP, red in A, white in A'; outlined) showed elevated *EcRE-lacZ* expression (green in A, white in A"). (B) *br* RNAi-misexpressing clones (red in B, white in B') of a late stage 9 egg chamber created by flip-out Gal4/UAS technique showed enhanced *EcRE-lacZ* expression (green in B, white in B"). Signal intensity was measured by the Interactive 3D Surface Plot Plugin (B'"). Anterior is to the left. Bars, 20 μm.

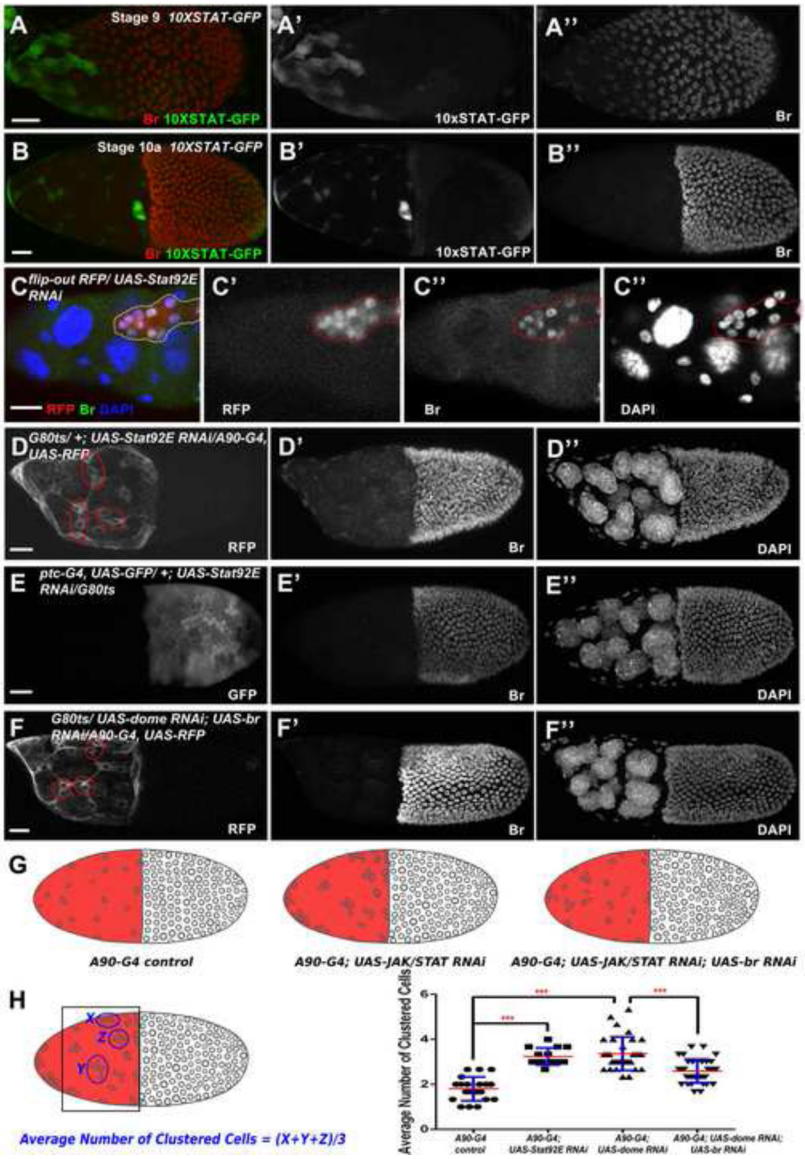

Figure 6.

JAK/STAT signaling downregulates Br in the SCs. (A-B) Expression of JAK/STAT signaling reporter *10XSTAT-GFP* showed an increased expression at stage 9 (green in A, white in A'), which is in contrast to decreased Br expression (red in A, white in A"). Moderate JAK/STAT activity persisted at stage 10a (green in B, white in B'), and no Br (red in B, white in B") was observed. (C) In the flip-out knockdown clones of a stage 10a egg chamber (red in C, white in C') of Stat92E, a key component of JAK/STAT signaling, SCs failed to disperse properly. (D) *Stat92E* RNAi-induced JAK/STAT downregulation driven by A90-Gal4 (white in D) caused accumulation of SCs in clusters of four to five cells, and showed elevated Br expression. (E) *Stat92E* RNAi-induced JAK/STAT downregulation in MbFCs (white in E) did not affect SC flattening and MbFC migration. (F) Introducing *br* RNAi in *domeless* RNAi-induced JAK/STAT-knockdown SCs partially restored proper SC dispersion, in clusters of around three cells. (G) Diagrams depict the distribution of

SCs in different genetic backgrounds. (H) The Average Number of Clustered Cells (ANCC) was applied to count the number of clustered SCs. Statistical differences of ANCC were observed between *A90-Gal4* control (n=20) and *A90-Gal4; UAS-JAK/STAT RNAi* (*Stat92E RNAi* and *dome RNAi*) groups (n=14 and 32, respectively), *A90-Gal4; UAS- dome RNAi* (n=32) and *A90-Gal4; UAS- dome RNAi; UAS-br RNAi* group (n=35). ***p<0.001. DAPI staining marks cell nuclei. Anterior is to the left. Bars, 20 μm.

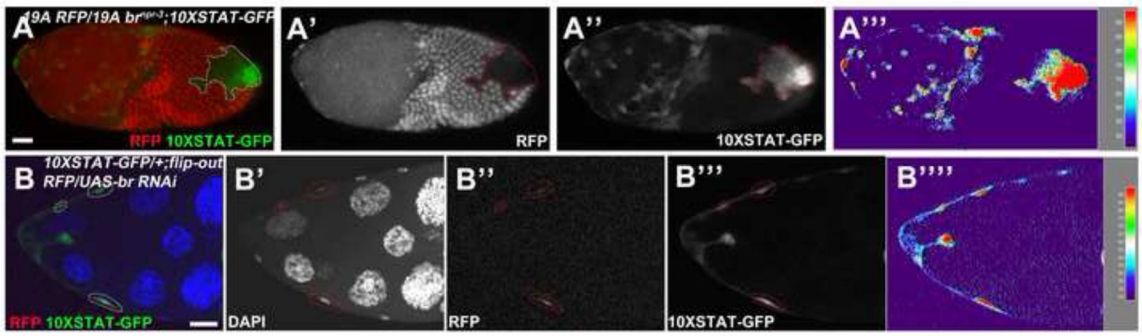

Figure 7.

Br feeds back to suppress JAK/STAT activity. (A) Stage 10a $br^{npr\text{-}3}$ follicle-cell clones (marked by the absence of RFP, red in A, white in A'; outlined) showed elevated *10XSTAT-GFP* expression (green in A, white in A"). (B) *br* RNAi-misexpressing clones (red in B, white in B") of a stage 10a egg chamber created by flip-out Gal4/UAS technique showed enhanced *10XSTAT-GFP* expression (green in B, white in B'"). Signal intensity was measured by the Interactive 3D Surface Plot Plugin (A'", B""). Anterior is to the left. Bars, 20 μm.

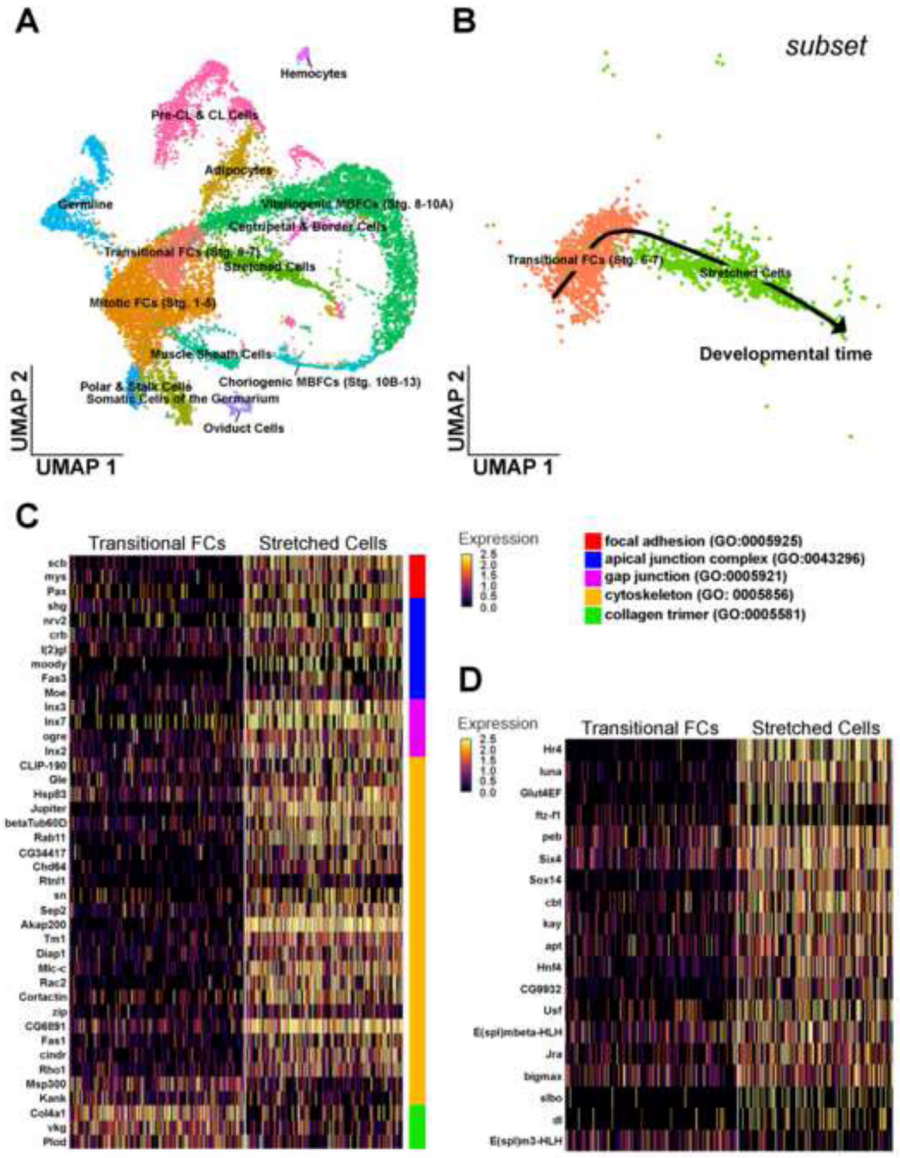

Figure 8.

Transcriptional patterns before and during cell stretching. (A) Uniform Manifold Approximation and Projection (UMAP) plot of wild-type RNA sequencing data with all clusters labeled according to cell type. (B) Subset UMAP containing just the transitional FCs (Stg. 6–7) and SCs. A black arrow overlay indicates the direction of developmental time. (C) Heatmap reporting the scaled expression of significant cell shape organization genes from differential expression analysis between the subset transitional FC and SC clusters. Genes are organized at right with colored bars indicating the GO term each gene belongs to. (D) Heatmap reporting the scaled expression of significant transcription factors from differential expression analysis between the subset transitional FC and SC clusters.

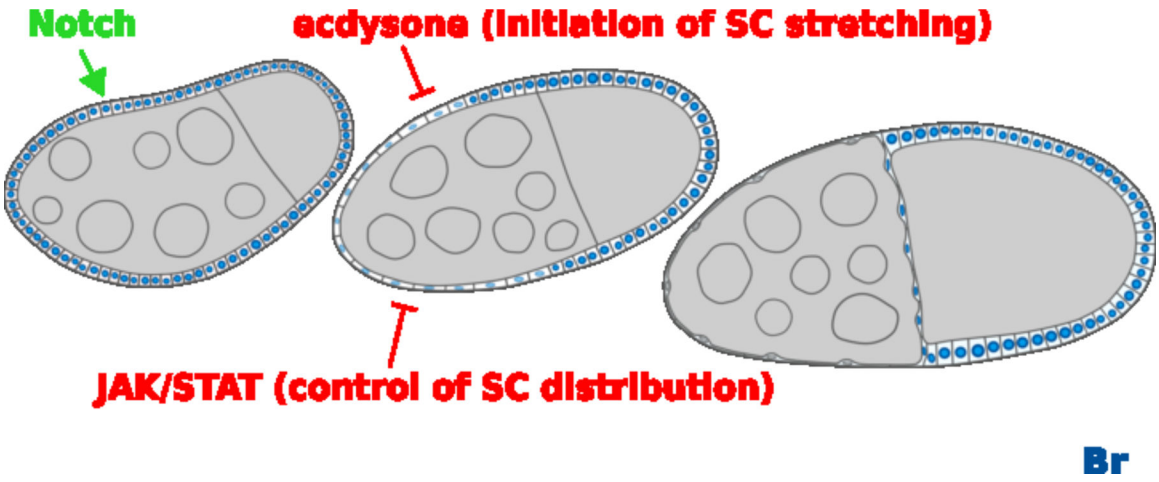

Figure 9.

Notch, ecdysone and JAK/STAT signaling regulates Br. Notch signaling induces and maintains Br expression from stages 5/6, ecdysone initiates the SC stretching while JAK/STAT signaling affects SCs distribution. DAPI staining marks cell nuclei. Anterior is to the left. Bars, 20 μm.